



Original Article

Sesquiterpene Lactones as Potential G1/S Phase Cell Cycle Inhibitors: A Molecular Docking Study

Zoufshan Yousaf¹, Aqsa Zaman¹, Muhammad Ali², Muhammad Khan^{1*}, Chaman Ara¹, Hafiz Abdullah Shakir¹, Muhammad Irfan³ and Bushra Nisar Khan¹¹Cancer Research Lab, Institute of Zoology, University of the Punjab, Quaid-e-Azam Campus, Lahore, Pakistan²National University of Medical Sciences (NUMS), Rawalpindi, Pakistan³Department of Biotechnology, University of Sargodha, Sargodha, Pakistan

ARTICLE INFO

Key Words:

Cyclin D1/ CDK4-CDK6, E2F-2, Sesquiterpene Lactones, Molecular Docking, Cell Cycle Arrest

How to Cite:

Yousaf, Z. ., Zaman, A., Ali, M. ., Khan, M. ., Ara, C. ., Shakir, H. A. ., Irfan, M., & Khan, B. N. . (2023). Sesquiterpene Lactones as Potential G1/S Phase Cell Cycle Inhibitors: A Molecular Docking Study: Sesquiterpene Lactones as Potential Cell Cycle Inhibitors. *Pakistan BioMedical Journal*, 6(08). <https://doi.org/10.54393/pbmj.v6i08.925>

*Corresponding Author:

Muhammad Khan

Cancer Research Lab, Institute of Zoology, University of the Punjab, Quaid-e-Azam Campus, Lahore, Pakistan

khan_zoologist@ymail.comReceived Date: 1st August, 2023Acceptance Date: 25th August, 2023Published Date: 31st August, 2023

ABSTRACT

Cell cycle checkpoints play a crucial role in cell division by monitoring the orderly progression of each phase, ensuring accurate completion before advancing to the next stage. They act as quality control mechanisms, pausing the cell cycle when optimal conditions are not met, thereby preventing errors during cell division. **Objective:** To discover Sesquiterpene Lactones (SLs) as inhibitory compounds targeting Cyclin D1/Cyclin Dependent Kinase 4 (CDK4)- Cyclin Dependent kinase 6 (CDK6) complex and Eukaryotic Transcription Factor 2 protein (E2F-2). **Methods:** The inhibitory potential of SLs, namely ilicol, eucalyptone, and ascleposide E, was investigated using molecular docking analysis. The docking and visualization of ligand-protein complexes were performed using MGL Tools version 1.5.7, BIOVIA Discovery Studio version 21.1.0, and PyMol version 2.5.2. Additionally, drug likeness and pharmacokinetic properties of SLs were assessed via pkCSM and ADMET analysis. **Results:** Findings demonstrate that ilicol exhibit most favourable complex with CDK6 having binding energy of -7.8 kCal/mol and inhibition constant 1.81 μ M. The visualization of ligand-receptor complexes reveals substantial hydrogen bonding interactions. **Conclusions:** Current study revealed that novel SLs show favourable drug likeness and promising ADMET profile along with strong inhibitory effect on G1/S regulatory proteins. The potency of SLs is in order of ilicol > ascleposide E > eucalyptone. To further validate the inhibitory effect of ilicol, implementation of comprehensive in vitro and in vivo investigations must be employed for progression of its development as a novel anti-cancer therapeutic.

INTRODUCTION

Cancer is a heterogenous disease which arise from uncontrolled proliferation of cells brought about by the dysregulation of cell cycle. Cancer continues to be a major cause of mortality worldwide, claiming millions of lives each year. The cell cycle is a highly regulated process that governs cell division and replication [1]. Cyclin D1, in conjunction with CDK4 and CDK6, plays a pivotal role in G1 phase by controlling the transition from G1 to S phase and initiating DNA synthesis and promoting cell proliferation. Inhibition of key proteins like CyclinD/CDK4-6 complex, can halt abnormal cell proliferation, promote cell cycle arrest,

and facilitate DNA repair or induce apoptosis [2-4]. The cyclin D/CDK4-CDK6 complex acts as a gatekeeper, ensuring that cell division proceeds only when the conditions are favourable. Cyclin D binds to CDK4 and CDK6, activating their kinase activity. Once activated, CDK4 and CDK6 phosphorylate and inactivate the retinoblastoma protein (pRb). This phosphorylation releases E2F transcription factors, which are essential for driving the expression of genes involved in DNA synthesis and cell cycle progression [3, 5]. By regulating the activity of the cyclin D/CDK4-CDK6 complex, the cell cycle

checkpoint ensures that cells pass the G1 phase only when sufficient growth signals, nutrient availability, and DNA integrity are present [6]. Inhibiting cyclin D, CDK4, CDK6, and E2F has become a promising approach for cancer treatment. By inhibiting the formation of cyclin D/CDK4-CDK6 complex, the phosphorylation of Rb is halted, leading to the restriction of E2F and subsequent inhibition of E2F-mediated gene transcription. As the expression of genes involved in DNA replication and cell cycle progression is reduced, it leads to cell cycle arrest and inhibition of cancer cell proliferation. This approach holds potential for developing targeted therapies that selectively suppress these proteins in cancer cells [5, 7, 8]. Plant compounds possess exhibit a lower risk of adverse effects and toxicity owed to their natural origin and evolutionary compatibility with human physiology. Secondly, the bioactive constituents in plant compounds can synergistically target multiple pathways and molecular targets involved in cancer progression, enhancing efficacy and minimizing the development of drug resistance [9-11, 1]. Sesquiterpene lactones are a class of natural compounds characterized by their 15-carbon ring structure and diverse biological activities. SLs exhibit notable anti-cancer activity, attributed to their ability to interfere with various cellular processes involved in tumor growth and metastasis [12, 13].

METHODS

Molecular docking is a computational analysis extensively used in drug discovery to predict the binding affinity and mode of interaction between a ligand and receptor. It comprises of multiple steps, including retrieval of protein and ligand structures, optimization of their conformations, docking of the ligand within the receptor's binding site, and subsequent evaluation of the resulting docked complexes. Notably, this technique facilitates the identification of optimal ligand-receptor orientations and interactions, aiding in design and optimization of potential therapeutic agents [14, 15]. The 3D crystal structures of G1/S cell cycle checkpoint proteins, including Cyclin D1 (PDB ID: 2W9Z), CDK4 (PDB ID: 1X02), CDK6 (PDB ID: 2W96), and E2F-2 (PDB ID: 1N4M), were retrieved from the RCSB Protein Data Bank (PDB). These protein structures underwent processing in AutoDock (AD), which involved steps such as removal of water molecules, addition of polar hydrogen, assignment of Kollman charges, and conversion to PDBQT format. Bioactive SL molecules, namely eucalyptone (CID: 91885002), ascleposide E (CID: 10668005), and ilicol (CID: 44559657), were obtained from PubChem and optimized for docking in PDBQT format. Semi-flexible docking was performed using AD, where the protein was kept rigid while the ligand was allowed to undergo conformational changes. Grid boxes, the docking search space centred

around the protein's active site, were set up using AD with specific dimensions, spacing (0.375), and size (40) for each protein. After generating multiple ligand conformations and ranking them based on binding energy, the conformation with the highest binding energy was selected as the most probable binding mode. Visualization of docked complexes and analysis of protein-ligand interactions were carried out using PyMol and BIOVIA Discovery Studio. To evaluate the pharmacokinetic properties of the investigated SLs, the online servers pkCSM and SwissADME were utilized. These tools provide an assessment of the Absorption, Distribution, Metabolism, Excretion, and Toxicity (ADMET) profiles for the potential lead compounds. Additionally, they evaluate drug likeness based on the Lipinski Rule of 5, which aids in predicting the absorption and permeability of small molecules and enables the identification of candidates with favorable pharmacokinetic properties. The SMILES notation of the selected ligands was obtained from PubChem and subjected to analysis using pkCSM [16, 17].

RESULTS

Binding energy represents the strength of interaction between a ligand (drug candidate) and a receptor (target protein). It provides an estimate of the stability and affinity of the ligand-receptor complex. A lower binding energy indicates a stronger interaction, suggesting a higher likelihood of successful binding. Inhibition constants reflect the concentration of the ligand required to achieve a given level of inhibition. A lower inhibition constant indicates a more potent inhibitor, as it implies a lower ligand concentration is needed to achieve a desired level of inhibition. The investigation of SL compounds in this study consistently revealed low binding energies and inhibition constants, emphasizing their potential as potent anti-cancer agents (Table 1).

Table 1: Characterization of binding energies and inhibition constants of novel SL drugs when bound to G1/S checkpoint proteins

Ligands (SLs)		CDK6	CDK4	Cuclin D1	E2F-2
Eucalyptone	Binding Energy (kcal/mol)	-6.7	-6.0	-7.2	-7.3
	Inhibition Constant (μ M)	11.69	38.32	5.01	4.23
Ilicol	Binding Energy (kcal/mol)	-7.8	-6.1	-7.1	-7.8
	Inhibition Constant (μ M)	1.81	32.34	5.93	1.81
Ascleposide E	Binding Energy (kcal/mol)	-7.1	-6.9	-7.0	-6.9
	Inhibition Constant (μ M)	5.93	8.33	7.03	8.33

Various types of protein-ligand interactions were observed by visualizing docked complexes. These interactions determine stability of ligand on protein's active site which can result in an effective protein inhibition. Binding energies and inhibition constants tend to decrease as a result of strong protein-ligand interactions. The most

observed interactions are hydrogen bonds, Van der Waals interactions, hydrophobic and electrostatic interactions. Among the SLs ilicol showed the strongest binding affinities in complex with CDK6 and E2F-2 of -7.8 kcal/mol and lowest inhibition constant $1.81\mu\text{M}$. The ilicol-CDK6 complex shows robust interactions including a hydrogen bond at residue VAL-150, bond distance of 2.44\AA . Additionally, the complex includes alkyl hydrophobic interactions with protein residues LEU-185(5.39\AA) VAL-77(5.32\AA)(Figure 1).

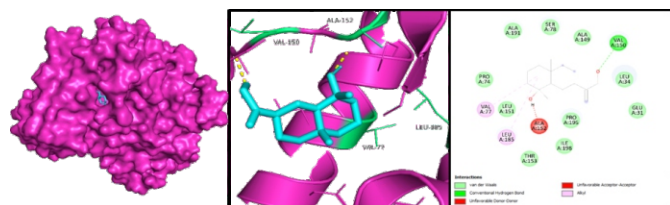


Figure 1: a) The complex between Ilicol and CDK6, highlighting the conformation of ligand to the protein's binding region; b) A three-dimensional representation illustrating interactions within the docking complex; and c) A two-dimensional visualization of the protein-ligand complex

Ilicol-E2F-2 complex is characterized by a hydrogen bond formed at residues ALA-152(2.13\AA) and two hydrogen bonds with the residue VAL-150(2.52\AA , 1.97\AA) and hydrophobic alkyl interactions at LEU-34 (5.10\AA), VAL-77 (5.31\AA), LEU-185(5.39\AA) and PRO-195(5.18\AA)(Figure 2).

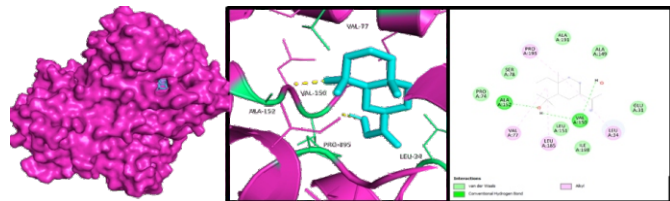


Figure 2: a) The Ilicol - E2F-2 complex, illustrating the binding of the ligand to the protein's binding region; b) a Figure 1: Three-dimensional depiction of the interactions within the docking complex; and c) Two-dimensional image showcasing the protein-ligand complex

Additionally, ilicol-cyclin D1 complex showed promising interactions including hydrogen bond with PHE-66(2.76\AA) residue and hydrophobic interactions at residues LEU-6 (5.15\AA), ALA-30(4.69\AA) and PHE-66(5.04\AA)(Figure 3).

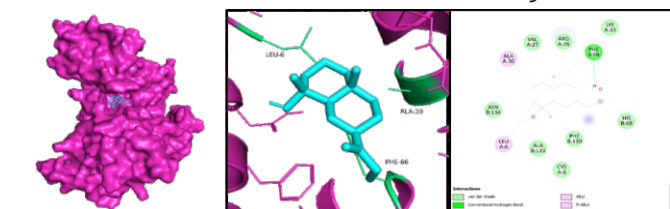


Figure 3: a) The binding of Ilicol to the Cyclin D1 protein in a complex, highlighting the ligand's occupancy in the protein's binding region; b) Three-dimensional representation portraying the interactions occurring within the docking complex; and c) Two-dimensional visualization illustrating the protein-ligand

complex

Ilicol, ascleposide E shows strong affinities with CDK4, CDK6 and cyclin D1 proteins. Ascleposide E-Cyclin D1 complex was observed to have six hydrogen bonds, three of them formed in interaction with residue ARG-26 with bond distances 2.92\AA , 2.82\AA and 2.20\AA . The rest of hydrogen bonds formed with LYS-33(1.81\AA), HIS-68(2.07\AA) and PHE-66(2.90\AA)(Figure 4).

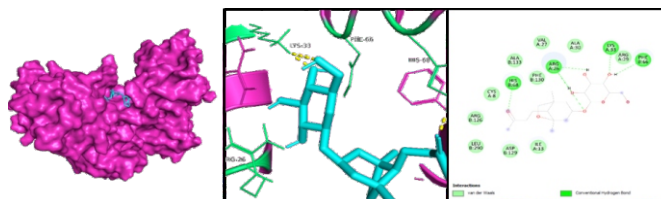


Figure 4: a) The complex between Ascleposide E and Cyclin D1, highlighting the binding of the ligand to the protein's binding region; b) A three-dimensional representation illustrating the interactions within the docking complex; and c) A two-dimensional visualization of the protein-ligand complex

Ascleposide E-CDK4 complex is distinguished by the presence of five hydrogen bonds created with residues ARG-87(2.32\AA), LYS-149(2.27\AA), LYS-147(2.78\AA) and ALA-39(1.95\AA and 2.12\AA)(Figure 5).

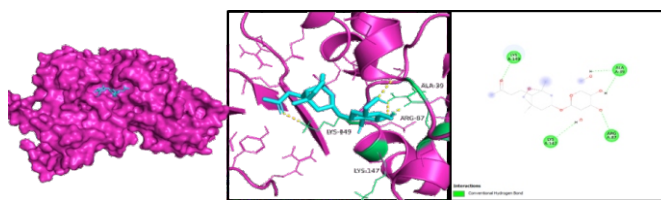


Figure 5: a) The Ascleposide E-CDK4 complex, illustrating the binding of the ligand to the protein's binding region; b) a Figure 1: Three-dimensional depiction of the interactions within the docking complex; and c) Two-dimensional image showcasing the protein-ligand complex

Ascleposide E-CDK6 complex is established by occurrence of seven hydrogen bonds at residues LYS-70 (2.15\AA), PHE-66 (2.07\AA), LYS-112 (2.46\AA , 2.17\AA and 2.76\AA) and GLU-67 (3.35\AA and 3.58\AA)(Figure 6).



Figure 6: a) The binding of Ascleposide E to the CDK6 protein in a complex, highlighting the ligand's occupancy in the protein's binding region; b) Three-dimensional representation portraying the interactions occurring within the docking complex; and c) Two-dimensional visualization illustrating the protein-ligand complex

Eucalyptone formed strong complexes with Cyclin D1 and E2F-2 displaying binding affinities -7.2 kcal/mol and -7.3

kcal/mol, respectively. Eucalyptone-Cyclin D 1 complex is characterized by four hydrogen bonds with active site residues ARG-26 (2.94Å and 2.80Å) and ARG-29 (2.68Å and 3.33Å). Hydrophobic pi-alkyl associations were observed at HIS-68 (5.26Å) and ILE-13 (5.42Å). Moreover, an electrostatic pi-anion interaction at residue ASP-129 (4.09Å) was also noticed in the complex, as depicted in Figure 7.

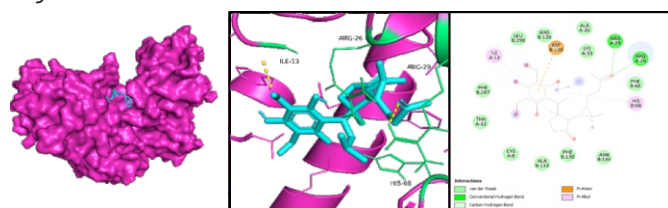


Figure 7: a) The Eucalyptone-Cyclin D 1 complex, illustrating the binding of the ligand to the protein's binding region; b) Three-dimensional depiction of the interactions within the docking complex; and c) Two-dimensional image showcasing the protein-ligand complex

The docking complex between eucalyptone and E2F-2 active site is characterized by five hydrogen bonds at residues AL-23 (2.41Å), TYR-24 (1.85Å), ARG-60 (2.08Å) and ARG-144 (2.05Å) along with a hydrophobic association at ALA-23 (3.15Å) (Figure 8).

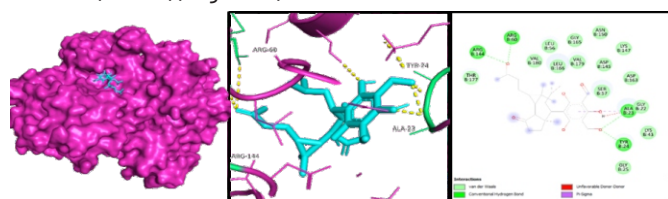


Figure 8: a) The binding of Eucalyptone to the E2F-2 protein in a complex, highlighting the ligand's occupancy in the protein's binding region; b) Three-dimensional representation portraying the interactions occurring within the docking complex; and c) Two-dimensional visualization illustrating the protein-ligand complex

The Lipinski Rule of 5 is employed in drug design to assess drug likeness based on specific molecular properties. It comprises of four key parameters: molecular weight, lipophilicity (logP), number of hydrogen bond donors, and number of hydrogen bond acceptors (Table 2).

Table 2: Assessment of drug-likeness for the novel SLs utilizing the pkCSM online database server

Ligands (SIs)	log P < 5	Molecular weight < 500 (g/mol)	H-bond acceptor < 10	H-bond donors < 5
Eucalyptone	5.1849	486.605	7	3
Illicol	2.8924	238.371	2	2
Ascleposide E	-0.2541	388.457	8	4

ADMET profiles are employed in drug design to assess and optimize the absorption, distribution, metabolism, excretion, and toxicity properties of potential drug candidates, ensuring their safety, efficacy, and overall

pharmacokinetic characteristics (Table 3).

Table 3: In-silico ADMET analysis of the novel SLs performed using SwissADME

ADMET	Parameters	Eucalyptone	Illicol	Ascleposide E
Absorbance	Water solubility (log S) mol/L	-3.977	-3.194	-2.938
	P-glycoprotein I/II inhibitor	Yes	No	No
	Intestinal absorption %	91.219	93.228	48.81
Distribution	log VDss (L/Kg)	0.068	0.306	-0.21
Metabolism	CYP2D6 substrate	No	No	No
	CYP2D6 inhibitor	No	No	No
	CYP3A4 substrate	Yes	No	No
	CYP3A4 inhibitor	No	No	No
Excretion	Total clearance (Log ml/min/kg)	0.24	1.129	1.142
	Renal OCT2 substrate	No	No	No
Toxicity	Hepatotoxicity	No	No	No
	AMES	No	No	No
	Maximum tolerable dose (log mg/kg/day)	-0.203	0.15	0.08

DISCUSSION

The aim of this study was to explore the anti-cancer properties of newly discovered plant-based compounds as inhibitors of the cyclin D/CDK4-CDK6 and E2F-2, using in-silico techniques. Our investigation demonstrated strong interactions between all three selected drug candidates and the residues of cyclin D1, CDK4, CDK6 and E2F-2, indicating their potential as inhibitors. Notably, illicol exhibited the highest binding affinity of -7.8 kcal/mol. Numerous reports have highlighted the anti-cancer potential of various SLs through the inhibition of G1/S phase regulatory proteins in different cancer cell lines, thereby suppressing cell proliferation. Several studies regarding britannin, a pseudoguaianolide SL, have shown its potential as an anti-cancer agent by inhibiting G1/S phase progression via downregulation of its regulatory proteins, cyclin D and CDK4 in human breast cancer MCF7 and MDA-MB468 cell lines and colon cancer HCT116 cell line [18, 19]. Recently, another SL alantolactone has gained attention as a promising anti-tumor drug due to its capacity to target multiple molecular pathways [20]. Alantolactone induces G1 phase cell cycle arrest in various cancer cell lines, such as squamous lung cancer SK-MES1 cells [21] and human myeloma cell lines RPMI-8226, MM1R, and NCI-H929 [22], by suppressing several proteins, including Cyclin D1, CDK4, and CDK6. Similarly, treatment of breast cancer MDA-MB231 cells with brevilin A SL compound resulted in reduced expressions of several protein like cyclin D1, CDK4 and CDK6, resulting in cell cycle arrest and apoptosis of cancer cells [23]. According to the Lipinski rule of 5, for a

compound to have favourable drug-like characteristics, it should have a molecular weight below 500 Dalton, a logP value not exceeding 5, no more than 5 hydrogen bond donors, and no more than 10 hydrogen bond acceptors [24]. These criteria are derived from the observation that compounds adhering to these thresholds often demonstrate improved oral absorption, permeability, and bioavailability. However, it is important to note that the Lipinski Rule of 5 is a guideline rather than an absolute rule, and deviations from these parameters can still result in successful drug candidates [25]. The molecular profile of the studied SLs aligns with all the guidelines (Table 2), except for the lipophilicity of eucalyptones, which was slightly higher ($\log P=5.18$) than the threshold ($\log P \leq 5.00$) defined by Lipinski's rule. The ADMET profile is of paramount importance in drug discovery as it provides essential insights into a drug properties, enabling optimization of potential therapeutic agents (Table 3). Absorbance is a critical parameter for evaluating the bioavailability and efficacy of a drug. Several parameters are considered to analyze absorbance, including water solubility ($\log S$) in mol/L, measuring the drug's ability to dissolve in aqueous solutions. Higher water solubility generally enhances absorbance. All the investigated SLs demonstrate effective absorbance at 25°C as they fall within the significant soluble $\log S$ range of -4 to -2 mol/L [26]. P-glycoprotein I/II is an efflux membrane transporter, upregulated in cancer cells and is responsible for impeding the absorption and bioavailability of chemotherapeutic drugs. P-glycoprotein I/II inhibitors have the potential to significantly enhance the uptake of anticancer drugs by several folds but they may also lead to adverse drug-drug interactions [27]. As demonstrated in Table 3, ilicol and ascleposide E are not P-glycoprotein I/II inhibitors however, eucalyptone being an inhibitor implicate higher drug absorbance at the risk of unfavorable pharmacokinetic interaction. All studied compounds show favorable intestinal absorption with absorbance $>90\%$ in case of eucalyptone and ilicol and 48% of ascleposide E, indicating efficient absorption compared to poorly absorbed molecules with values $<30\%$ [28]. The distribution parameter $\log V_{Dss}$ (volume of distribution at steady state) represents the extent of drug distribution throughout the body, ensuring a uniform concentration in the blood plasma [29]. The ideal V_{Dss} belongs within the range of -0.15 to 0.45 [30], as depicted in table 3, ascleposide E falls outside the range having low ($\log V_{Dss} = -0.21$ L/Kg) distribution value, on the other hand, ilicol and eucalyptone exhibit optimal V_{Dss} values. Cytochrome P450 (CYP450) is a family of enzymes found in the liver and other tissues that play a vital role in the metabolism of drugs and endogenous compounds. CYP450 isoforms, CYP3A4 and

CYP2D6, are involved in the biotransformation of numerous drugs by oxidizing or modifying their chemical structures [30]. It is crucial to carefully evaluate the potential implications of CYP interactions, as they can lead to adverse effects or altered pharmacokinetics when combined with other medications [31]. Table 3 demonstrate that SLs show no significant interaction with CYP isoforms as either substrate or inhibitor, apart from eucalyptone having potential of being CYP3A4 substrate which can have both positive and negative implications. Being a substrate of CYP3A4 enzyme can facilitate the pronounced clearance and elimination of drug from body. However, it can also pose a challenge by potentially causing drug-drug interactions due to elevated enzyme activity and broad substrate specificity [32]. Renal OCT2 substrate relates to the drug's interaction with the organic cation transporter 2 (OCT2) in the kidney, which plays a significant role in the renal elimination of drugs and its metabolites from body. If a drug is identified as a Renal OCT2 substrate, it suggests that it undergoes active transport by OCT2 from the bloodstream into the urine, contributing to its excretion. All SLs under consideration are not renal OCT2 substrate which may prove advantageous as it can lead to reduced clearance consequently, increased drug concentrations and enhanced therapeutic effects but raise the risk of toxicity and drug interactions [31, 33]. Total clearance represents the sum of all clearance mechanisms that remove the drug from the systemic circulation [33]. Ilicol and ascleposide E have high total clearance values, 1.129 and 1.142 \log ml/min/kg meaning these compounds are eliminated rapidly from body. AMES toxicity analysis is a bacterial mutagenicity assay that assesses drug's potential to induce genetic mutations [31, 34]. The early identification of mutagenic potential in compounds during drug discovery holds paramount significance, as it enables the prevention of the development of harmful drugs. All of the compounds studied exhibit a lack of mutagenic potential. Hepatotoxicity is the drug's potential to cause liver damage or dysfunction. All the SLs are non-hepatotoxic thus pose no danger to liver tissues. Maximum tolerable dose is the highest dose that can be administered to a patient without causing unacceptable or severe adverse effects [33, 34]. Given that all three compounds possess a maximum tolerable dose below 0.477 \log mg/kg/d [33], they can be deemed highly potent even at low concentrations, surpassing this limit may lead to potential toxicity.

CONCLUSIONS

Our study focused on investigating sesquiterpene lactones that specifically target the Cyclin D1/CDK4-6 protein complex and E2F-2, with the objective of inducing cell cycle

arrest at the G1/S phase. Through rigorous molecular docking analysis, we identified ilicol, ascleposide E and eucalyptone as compounds exhibiting substantial inhibition potential. These compounds demonstrated favourable hydrogen and hydrophobic interactions, which are critical for their inhibitory activity. To further validate and enhance our understanding of their inhibitory effects, we propose conducting comprehensive in vitro experiments. These experiments will provide crucial insights into the compounds' effectiveness as G1/S phase inhibitors, thereby advancing their potential as novel therapeutic agents. By assessing the compounds' activity against relevant biological targets and evaluating their impact on cell cycle regulation, we aim to obtain valuable information that will inform future research endeavors and optimize their therapeutic efficacy.

Authors Contribution

Conceptualization: MK

Methodology: AZ, ZY, MI

Formal analysis: AZ, ZY, MA

Writing-review and editing: MK, CA, HAS, BNK

All authors have read and agreed to the published version of the manuscript.

Conflicts of Interest

The authors declare no conflict of interest.

Source of Funding

The authors received no financial support for the research, authorship and/or publication of this article.

REFERENCES

- [1] Khan M, Maryam A, Zhang H, Mehmood T, Ma T. Killing cancer with platycodin D through multiple mechanisms. *Journal of Cellular and Molecular Medicine*. 2016 Mar; 20(3): 389-402. doi: 10.1111/jcmm.12749.
- [2] Akçay Nİ, Nagy B, Tüzmen Ş. Reaction systems for modeling and validation of biological signaling pathways: G1/s checkpoint of the cell cycle. *Acta Polytechnica Hungarica*. 2021 Jan; 18(6): 7-23. doi: 10.12700/APH.18.6.2021.6.1.
- [3] Fischer M, Schade AE, Branigan TB, Müller GA, DeCaprio JA. Coordinating gene expression during the cell cycle. *Trends in Biochemical Sciences*. 2022 Dec; 47(12): 1009-1022. doi: 10.1016/j.tibs.2022.06.007.
- [4] Hassan SH, Gul S, Zahra HS, Maryam A, Shakir HA, Khan M, et al. Alpha solanine: A novel natural bioactive molecule with anticancer effects in multiple human malignancies. *Nutrition and Cancer*. 2021 Aug; 73(9): 1541-52. doi: 10.1080/01635581.2020.1803932.
- [5] Nardone V, Barbarino M, Angrisani A, Correale P, Pastina P, Cappabianca S, et al. CDK4, CDK6/cyclin-D1 complex inhibition and radiotherapy for cancer control: a role for autophagy. *International Journal of Molecular Sciences*. 2021 Aug; 22(16): 8391. doi: 10.3390/ijms22168391.
- [6] Limas JC and Cook JG. Preparation for DNA replication: the key to a successful S phase. *FEBS Letters*. 2019 Oct; 593(20): 2853-67. doi: 10.1002/1873-3468.13619.
- [7] Goel S, Bergholz JS, Zhao JJ. Targeting CDK4 and CDK6 in cancer. *Nature Reviews Cancer*. 2022 Jun; 22(6): 356-72. doi: 10.1038/s41568-022-00456-3.
- [8] Xiong Y, Li T, Assani G, Ling H, Zhou Q, Zeng Y, et al. Ribociclib, a selective cyclin D kinase 4/6 inhibitor, inhibits proliferation and induces apoptosis of human cervical cancer in vitro and in vivo. *Biomedicine & Pharmacotherapy*. 2019 Apr; 112: 108602. doi: 10.1016/j.biopha.2019.108602.
- [9] Newman DJ and Cragg GM. Natural products as sources of new drugs over the nearly four decades from 01/1981 to 09/2019. *Journal of Natural Products*. 2020 Mar; 83(3): 770-803. doi: 10.1021/acs.jnatprod.9b01285.
- [10] Khan M, Maryam A, Qazi JI, Ma T. Targeting apoptosis and multiple signaling pathways with icariside II in cancer cells. *International Journal of Biological Sciences*. 2015 Jul; 11(9): 1100. doi: 10.7150/ijbs.11595.
- [11] Pezzani R, Salehi B, Vitalini S, Iriti M, Zuñiga FA, Sharifi-Rad J, et al. Synergistic effects of plant derivatives and conventional chemotherapeutic agents: an update on the cancer perspective. *Medicina*. 2019 Apr 17; 55(4): 110. doi: 10.3390/medicina55040110.
- [12] Gou J, Hao F, Huang C, Kwon M, Chen F, Li C, Liu C, Ro DK, Tang H, Zhang Y. Discovery of a non-stereoselective cytochrome P450 catalyzing either 8 α - or 8 β -hydroxylation of germacrene A acid from the Chinese medicinal plant, *Inula hupehensis*. *The Plant Journal*. 2018 Jan; 93(1): 92-106. doi: 10.1111/tpj.13760.
- [13] Shams A, Ahmed A, Khan A, Khawaja S, Rehman NU, Qazi AS, et al. Naturally Isolated Sesquiterpene Lactone and Hydroxyanthraquinone Induce Apoptosis in Oral Squamous Cell Carcinoma Cell Line. *Cancers*. 2023 Jan; 15(2): 557. doi: 10.3390/cancers15020557.
- [14] Fan J, Fu A, Zhang L. Progress in molecular docking. *Quantitative Biology*. 2019 Jun; 7: 83-89. doi: 10.1016/bs.pmch.2021.01.004.
- [15] Stanzione F, Giangreco I, Cole JC. Use of molecular docking computational tools in drug discovery.

- Progress in Medicinal Chemistry. 2021 Jan; 60: 273-343. doi: 10.1016/bs.pmch.2021.01.004.
- [16] Kar S and Leszczynski J. Open access in silico tools to predict the ADMET profiling of drug candidates. *Expert Opinion on Drug Discovery*. 2020 Dec; 15(12): 1473-87. doi: 10.1080/17460441.2020.1798926.
- [17] Beck TC, Springs K, Morningstar JE, Mills C, Stoddard A, Guo L, et al. Application of Pharmacokinetic Prediction Platforms in the Design of Optimized Anti-Cancer Drugs. *Molecules*. 2022 Jun; 27(12): 3678. doi: 10.3390/molecules27123678.
- [18] Hamzeloo-Moghadam M, Aghaei M, Madi MH, Fallahian F. Anticancer activity of britannin through the downregulation of cyclin D1 and CDK4 in human breast cancer cells. *Journal of Cancer Research and Therapeutics*. 2019 Jul; 15(5): 1105-8. doi: 10.4103/jcrt.JCRT_517_17.
- [19] Zhang YF, Zhang ZH, Li MY, Wang JY, Xing Y, Ri M, et al. Britannin stabilizes T cell activity and inhibits proliferation and angiogenesis by targeting PD-L1 via abrogation of the crosstalk between Myc and HIF-1 α in cancer. *Phytomedicine*. 2021 Jan; 81: 153425. doi: 10.1016/j.phymed.2020.153425.
- [20] Khan M, Li T, Ahmad Khan MK, Rasul A, Nawaz F, Sun M, et al. Alantolactone induces apoptosis in HepG2 cells through GSH depletion, inhibition of STAT3 activation, and mitochondrial dysfunction. *BioMed Research International*. 2013 Oct; 2013: 719858. doi: 10.1155/2013/719858.
- [21] Zhao P, Pan Z, Luo Y, Zhang L, Li X, Zhang G, et al. Alantolactone induces apoptosis and cell cycle arrest on lung squamous cancer SK-MES-1 cells. *Journal of Biochemical and Molecular Toxicology*. 2015 May; 29(5): 199-206. doi: 10.1002/jbt.21685.
- [22] Yao Y, Xia D, Bian Y, Sun Y, Zhu F, Pan B, et al. Alantolactone induces G1 phase arrest and apoptosis of multiple myeloma cells and overcomes bortezomib resistance. *Apoptosis*. 2015 Aug; 20: 1122-33. doi: 10.1007/s10495-015-1140-2.
- [23] Qu Z, Lin Y, Mok DK, Bian Q, Tai WC, Chen S. Brevilin A, a natural sesquiterpene lactone inhibited the growth of triple-negative breast cancer cells via Akt/mTOR and STAT3 signaling pathways. *OncoTargets and Therapy*. 2020 Jun; 13: 5363-73. doi: 10.2147/OTT.S256833.
- [24] Lipinski CA. Lead-and drug-like compounds: the rule-of-five revolution. *Drug discovery today: Technologies*. 2004 Dec; 1(4): 337-41. doi: 10.1016/j.ddtec.2004.11.007.
- [25] Shultz MD. Two decades under the influence of the rule of five and the changing properties of approved oral drugs: miniperspective. *Journal of Medicinal Chemistry*. 2018 Sep; 62(4): 1701-14. doi: 10.1021/acs.jmedchem.8b00686.
- [26] Kuang Y, Shen W, Ma X, Wang Z, Xu R, Rao Q, Yang S. In silico identification of natural compounds against SARS-CoV-2 main protease from Chinese Herbal Medicines. *Future Science OA*. 2023 May; 9(7): FS0873. doi: 10.2144/fsoa-2023-0055.
- [27] Nguyen TT, Duong VA, Maeng HJ. Pharmaceutical formulations with P-glycoprotein inhibitory effect as promising approaches for enhancing oral drug absorption and bioavailability. *Pharmaceutics*. 2021 Jul; 13(7): 1103. doi: 10.3390/pharmaceutics13071103.
- [28] Llorach-Pares L, Nonell-Canals A, Sanchez-Martinez M, Avila C. Computer-aided drug design applied to marine drug discovery: Meridianins as Alzheimer's disease therapeutic agents. *Marine Drugs*. 2017 Nov; 15(12): 366. doi: 10.3390/md15120366.
- [29] Dharmasaputra A and Rasyida AU. Azasterol Inhibition and Pharmacokinetic Effects on Thymidylate Synthase-Dihydrofolate Reductase from *T. gondii*: In Silico Study. *Pharmacognosy Journal*. 2022 Jun; 14(3): 571-75. doi: 10.5530/pj.2022.14.73.
- [30] Wahyuningsih D, Purnomo Y, Tilaqza A. In Silico study of Pulutan (*Urena lobata*) leaf extract as anti-inflammation and their ADME prediction. *Journal of Tropical Pharmacy and Chemistry*. 2022 Jun; 6(1): 30-37. doi: 10.25026/jtpc.v6i1.323.
- [31] Muhammad S, Hassan SH, Al-Sehemi AG, Shakir HA, Khan M, Irfan M, Iqbal J. Exploring the new potential antiviral constituents of *Moringa oleifera* for SARS-CoV-2 pathogenesis: An in silico molecular docking and dynamic studies. *Chemical Physics Letters*. 2021 Mar; 767: 138379. doi: 10.1016/j.cplett.2021.138379.
- [32] Zhou SF. Drugs behave as substrates, inhibitors and inducers of human cytochrome P450 3A4. *Current Drug Metabolism*. 2008 May; 9(4): 310-22. doi: 10.2174/138920008784220664.
- [33] Bucuo XE and Solidum JN. In Silico Evaluation of Antidiabetic Activity and ADMET Prediction of Compounds from *Musa acuminata* Colla Peel. *Philippine Journal of Science*. 2022 Feb; 1: 171-92. doi: 10.56899/151.01.13.
- [34] Flores-Holguin N, Frau J, Glossman-Mitnik D. Computational Pharmacokinetics Report, ADMET Study and Conceptual DFT-Based Estimation of the Chemical Reactivity Properties of Marine Cyclopeptides. *ChemistryOpen*. 2021 Nov; 10(11): 1142-9. doi: 10.1002/open.202100178.